Available online at www.sciencedirect.com
ScienceDirect
Trans. Nonferrous Met. Soc. China 25(2015) 2156−2164
Transactions of Nonferrous Metals Society of China
www.tnmsc.cn

In situ analysis of multi-twin morphology and growth using synchrotron polychromatic X-ray microdiffraction

Li LI[1, 2]

1. Institute of Advanced Manufacturing Technology, Hunan Institute of Technology, Hengyang 421002, China;
2. Institute for Frontier Materials, Deakin University, Geelong, Victoria 3220, Australia

Received 1 September 2014; accepted 11 March 2015

Abstract: Synchrotron polychromatic X-ray microdiffraction (micro-XRD) was applied to study in situ deformation twinning of commercially AZ31 (Mg−3Al−1Zn) strip subjected to uniaxial tension. The morphology and growth of twins were analyzed in situ under the load level from 64 to 73 MPa. The X-ray microdiffraction data, collected on beamline 12.3.2 at the Advanced Light Source, were then used to map an area of 396 μm × 200 μm within the region of interest. The experimental set-up and X-ray diffraction microscopy with a depth resolution allow the position and orientation of each illuminated grain to be determined at the submicron size. A list of parent grains sorted by crystallographic orientation were selected to examine their twinning behavior. The results depict twin variant selection, local misorientation fluctuation and mosaic spread for multi-twins within the same parent grain. As load increases, the amplitude of misorientation fluctuation along twin trace keeps increasing. This is attributable to the accumulation of geometrically necessary dislocations.

Key words: synchrotron polychromatic X-ray; deformation twinning; in situ analysis; local misorientation; geometrically necessary dislocations

1 Introduction

Magnesium alloy, known as one of the lightest structural metallic materials, is getting more attractive in applications for the automotive and aerospace industries due to its low density and high specific strength. For the hexagonal-close-packed (HCP) structure aggregates, improved understanding of twinning is needed to enhance performance and give automotive makers confidence to use the metal more widely. Magnesium fails via mechanisms that involve deformation twinning. Unlike dislocation slipping process that is thermally activated function of temperature and strain rate, twinning process is stressfully activated and less sensitive to two factors above [1].

Post-mortem analysis of deformed structures has shed important light on the complexity of deformation twinning behaviors in HCP metals [2,3]. However, to understand twinning, in-situ characterization techniques are required to capture the onset and growth of twins, because a detectable drop in the volume fraction of twins is often observed with the release of load [4]. In-situ neutron diffraction has been widely employed to reveal important features of the average deformation behavior of embedded grains in metals deforming by twinning, and this has mostly been done for magnesium alloy [5]. However, more dedicated experimental study is required to investigate the yielding on the micro scale. MURÁNSKY et al [6] using in-situ neutron diffraction coupled with elasto-plastic self-consistent model demonstrated that critical resolved shear stress for the onset of twinning is found to exceed that for basal slip by a factor of 2−6 times. Therefore, it is implied that what happens prior to twin's onset and during twin's growth was "micro" yielding and hardening due to dislocation slip activities.

In line with these demands, the recent advances in synchrotron X-ray microdiffraction methods provide a new opportunity to nondestructively study the microtexture with sub-grain resolution [7]. The emerging 3DXRD crystal microscopes use synchrotron X-ray sources and advanced X-ray optics to probe polycrystalline materials with submicron X-ray beams.

Foundation item: Project (DP140102355) supported by the Australian Research Council (ARC); Project supported by the China Scholarship Council (CSC)
Corresponding author: Li LI; Tel/Fax: +86-734-3452030: E-mail: lileewin@163.com
DOI: 10.1016/S1003-6326(15)63827-4

Three dimensional distributions of the local crystalline phase, orientation (texture) and elastic strain tensor and geometrically necessary dislocation (GND) density tensor distributions can be measured with submicron resolution in all directions. Utilizing monochromatic high-energy 3DXRD measurements and grain reconstruction algorithms, AYDINER et al [8] presented the full stress tensor and its evolution in a growing deformation twin and corresponding parent grain. An alternative methodology known as polychromatic micro-XRD offers superior resolution for assessing intragranular microstructural information [9,10]. BALOGH et al [11] measured the strain gradients across a grain containing twins located in the bulk of a polycrystalline AZ31 sample, using the technique of different-aperture X-ray microscopy (DAXM) in polychromatic mode. ODDERSHEDE et al [12] measured the stress field around an evolving crack in tensile deformed Magnesium AZ31 using three dimensional X-ray diffraction. The insights into the spatial variant in material response and mechanical field localization gained from above direct measurement can lead to the development of more physically based predictive models.

In polycrystalline metallic aggregates, the nucleation and propagation of a twin produces a considerable shift of local elastic-plastic behavior of parent grain and needs to accommodate lattice rotations within twin. ASHBY [13] first pointed out the fundamental difference between homogeneous plastic deformation that can be accommodated by an arbitrary distribution of statistically stored dislocations (SSDs) and non-homogeneous plastic deformation that requires the particular distributions of GNDs to accommodate plastic strain gradients. The introduction of GNDs, in addition to the inherently random SSDs, results in increased hardening of the material. Twin formation and GND density strongly depend on initial microstructure and load directions [14]. PROUST et al [15] proposed an upgraded visco-plastic self-consistent model explicitly describing hardening in twin via GNDs and a directional Hall-Petch mechanism.

The modeling efforts need to be validated by experiment. From the experiments performed on a polycrystalline AZ31 sample, the objective of the present work is to provide a direct assessment of the micro-orientation and GNDs distribution within ongoing twins furnished from polychromatic micro-XRD.

2 Experimental

2.1 Experimental procedure

The material used is commercial AZ31 alloy sheet, rolled to a thickness of 1 mm and processed under half hard conditions. The tensile samples, prepared in accordance with ASTM E8 with a gauge length of 16 mm, were annealed at 400 °C for 1 h to reduce the residual stresses developed during fabrication. This heat treatment developed an equiaxed microstructure with an average grain size of 30 μm. It is confirmed by EBSD experiment that the initial texture of the rolled sheet is the conventional one in which most of the *c*-axis was aligned toward the normal direction, and that the initial microstructure was free of twin boundaries.

To perform in situ uniaxial tensile loading experiments, a deformation stage, previously used for micro-XRD studies, was utilized [16]. The loading system provided accurate control and feedback of the loading parameters necessary to re-create the macroscopic stress–strain curve. The tensile experiment was carried out under displacement control at the rate of 0.016 mm/s.

Figure 1 shows the schematic of the X-ray Laue-diffraction 3D microscope. The AZ31 magnesium sample was fixed in a tension jig. The tension direction was parallel to the rolling direction and in the tilt angle of 30° to the beam incident direction. A set of fixed right handed sample coordinates, of which the *z*-axis was

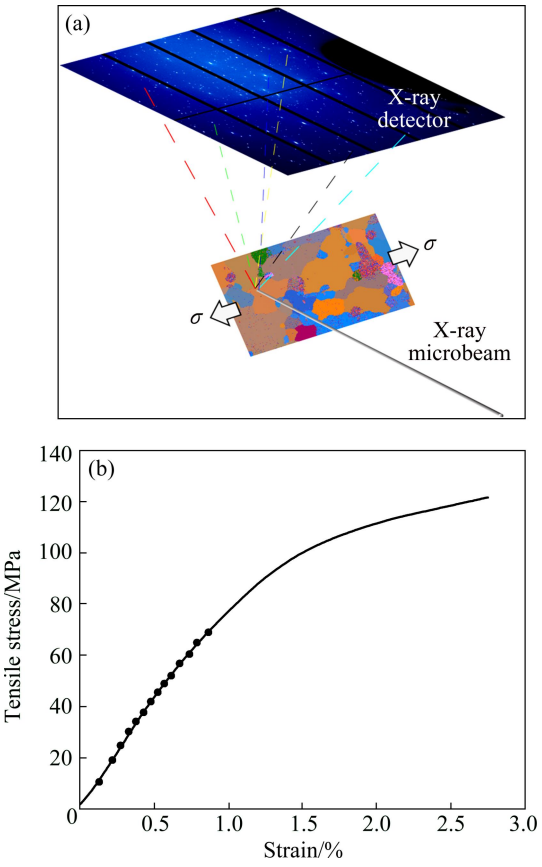

Fig. 1 Schematic of X-ray Laue-diffraction 3D microscope (a) and stress−strain curve for alloy (b) [16] (Points in Fig. 1(b) are indicative of macroscopic load at which micro-XRD maps were collected)

defined normal to the sample surface and the *x*-axis within the sample surface and perpendicular to the X-ray beam direction, was established for crystal orientation representation.

To ensure the exactly same positions on the specimen throughout the loading, the polycrystalline AZ31 sample was electrochemically polished and a series of fiducial markers in the form of micro-scale indents were introduced on the surface to define the region of interest [10]. Synchrotron X-ray microdiffraction measurements were performed on beam line 12.3.2 at the Advanced Light Source. The beamline utilizes an orthogonal pair of Kirkpatrick-Baez mirrors to focus polychromatic X-rays to a sub-micron spot (0.8 μm × 0.8 μm) with a penetration depth of 500−600 μm. Prior to data collection, a Laue patter (LP) collected from a strain free single crystal Si was used to precisely calibrate the experimental geometry that includes the sample-to-detector distance, the detector tilt angles, and the central channel position of the detector. After the region of interest was located, a small raster scan was performed on the area of 396 μm × 200 μm. The sample was translated across the beam in *X* and *Y* directions with the step lengths of 12 μm and 20 μm, respectively, generating an *XY* diffraction map from a specific region with 340 steps (34 × 10). Each step took 1s for exposure. At each step increment, the polychromatic Laue data were collected with a large area X-ray charge coupled detector (MAR133 CCD).

The white beam was focused using Kirkpatrick-Baez mirrors to a spot size of <1 μm^2 onto the sample. The sample was translated across the beam in *X* and *Y* directions with the step lengths of 12 μm and 20 μm, respectively, generating an *XY* diffraction map from a specific region. Therefore, the minimum spatial resolution was about 12 μm. Figure 2 shows the illustration for the minimum spatial resolution in this technique. When two twins form parallel as well as close to each other, it is possible to treat the two as one larger twin, as shown in Fig. 2(a). When the long axis of the twin is shorter than 20 μm, it is possible to omit it in this technique, as shown in Fig. 2(b).

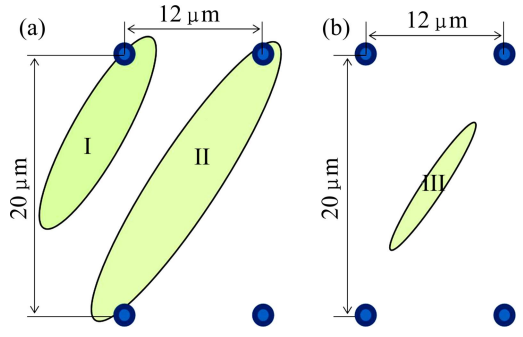

Fig. 2 Illustration for minimum spatial resolution

2.2 Twin indexation

X-ray microdiffraction analysis software (XMAS) developed by TAMURA et al [17,18] was used to analyze the X-ray microdiffraction images. The diffraction peak positions were determined by fitting two-dimensional Gaussian to individual crystalline reflections. All Laue diffraction patterns of grains at the nominal load of 12 MPa were automatically indexed with hexagonal lattice parameters (a=b=0.3209 nm, c=0.5210 nm, α=β=90°, γ=120°). The analysis results of XMAS were described by incident position, crystal orientation, strain, diffraction intensities for indexed (*hkl*) Laue reflections. The loading from 12 MPa to 73 MPa included 13 stages. As the load increased, the spread of the diffraction spots was recorded at the area detector that signifies the onset of plastic deformation.

Figure 3 displays the flow chart of twin indexation by analyzing micro-XRD data. The first step was to select the target grain as potential parent. When indexing the target grain, its orientation matrix including 9 elements was obtained, as shown in the following equation.

Parent orientation matrix=

$$\begin{bmatrix} 0.0686 & -0.0816 & -0.3023 \\ -0.0927 & 0.2992 & 0.0697 \\ 0.4970 & 0.1370 & 0.0763 \end{bmatrix} \begin{matrix} \rightarrow a1 \\ \rightarrow a2 \\ \rightarrow c \end{matrix}$$

In fact, one can automatically index points on different layers up to six grains in depth. When the orientation matrices of indexed spots matched with the matrix of target grain (i.e., the deviations of all corresponding elements were below 0.03), one affirms

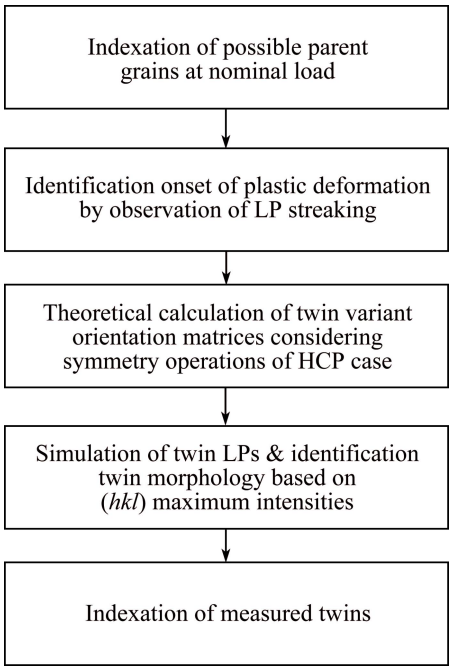

Fig. 3 Flow chart of twin indexation using micro-XRD data

that the points belong to the domain of target grain. Therefore, the orientation matrix can be regarded as the unique characteristic. In this way, one can obtain the morphology of target grain.

The second step was to observe the diffraction spots of the potential parent. If the diffraction spots are split by the intensity vacancy, the parent probably has twinned. Figure 4 illustrates the observation of intensity vacancy in one parent spot.

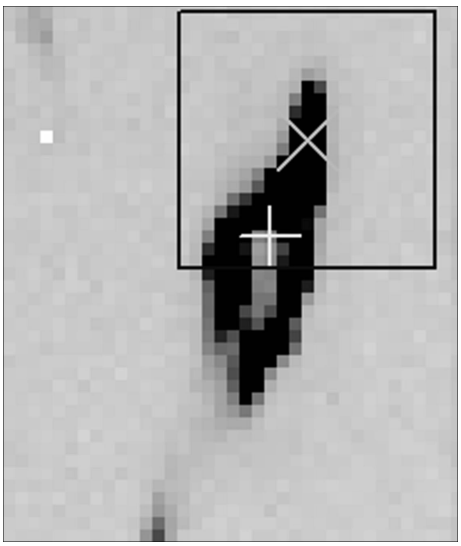

Fig. 4 Observing intensity vacancy in parent spot

The third step was to simulate the Laue pattern of theoretic twin, using the misorientation to the potential parent. From the orientations of potential parent grains, theoretical orientations of twin variant were calculated considering HCP symmetry operations. Based on the theoretical calculation, twin's LPs were simulated and compared with the experimental LPs. Because diffraction signals from twins are relatively weaker than those from the matrix, twin's LPs can not be indexed automatically. The fourth step was to index the twin and determine the twin's variant. In this way, one can figure out the morphology of twin. It has to be mentioned that twin is definitely confined within the parent, when comparing the morphology between parent and its twin.

Two-dimensional Gaussian method was used to fit the intensity of diffraction spot. The position of fitted maximum intensity was viewed as actual center of the spot. When one of potential (*hkl*) reflections from twin was determined, one can examine its maximum intensity distribution within the detected area. It should be mentioned that some of spots need to be excluded from indexation due to the broadening and fragmentation of Laue spots which arises from increased lattice orientation spread within the scattering volume. As a consequence, there are inevitably some Laue spots that can not be indexed. Considering the completeness of twin's diffraction spot, at least 10 spots can be identified. For each target parent grain or twin, there always are several Laue spots that exist in the reflection list for all indexed images. One of (*hkl*) intensity was selected to map the morphology of twin.

The precise shape of each Laue spot depends formally on the distribution of local orientations within the probed grain or subgrain volume. The streaking direction is directly related to the lattice curvature and GNDs density tensor. The length of the streak at the full width at half maximum is proportional to the total number of GN dislocations and boundaries within the probed region [19].

3 Results and discussion

3.1 Twin determination

Figure 5 presents the orientations of the twinned parent grains in the form of inverse pole figure. The convention for grain label is "position No. # layer depth" at nominal load. Within the scanning region, 33 grains were detected in different depth, but only 8 parent grains produced at least 14 twins. Moreover, the twinned parents posed an obvious tendency that they oriented the *c* axis parallel to the σ direction. From a list of 8 grains that located on the different depths, the parent involving three twins was selected for monitoring, i.e., parent 192#1.

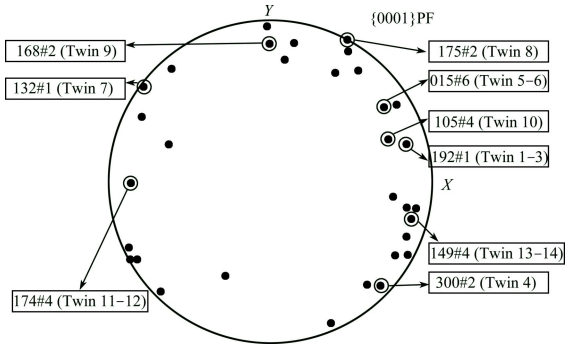

Fig. 5 Orientations of identified grains (dark spots) and twinned parent grains (dark spots in circles)

Figures 6(a) and (b) illustrate the crystallographic indexation of twins 1−3 and their parent grain at the position of x=10142 μm, y=−5910 μm for the load stage of 68 MPa. For the purpose of clarity, not all indexations are presented. It is shown that twin's Laue spots are basically round with relatively low intensity compared with those of parent grain with highly localized plastic deformation which is identified by severe streaking. Based on the indexation, the misorientation between parent and twins was calculated as 86.1° ⟨−0.159 0.321 −0.161 0.001⟩, i.e., tensile twin $\{10\bar{1}2\}\langle 10\bar{1}1\rangle$ with the ideal misorientation of 86.4° $\langle \bar{1}2\bar{1}0\rangle$.

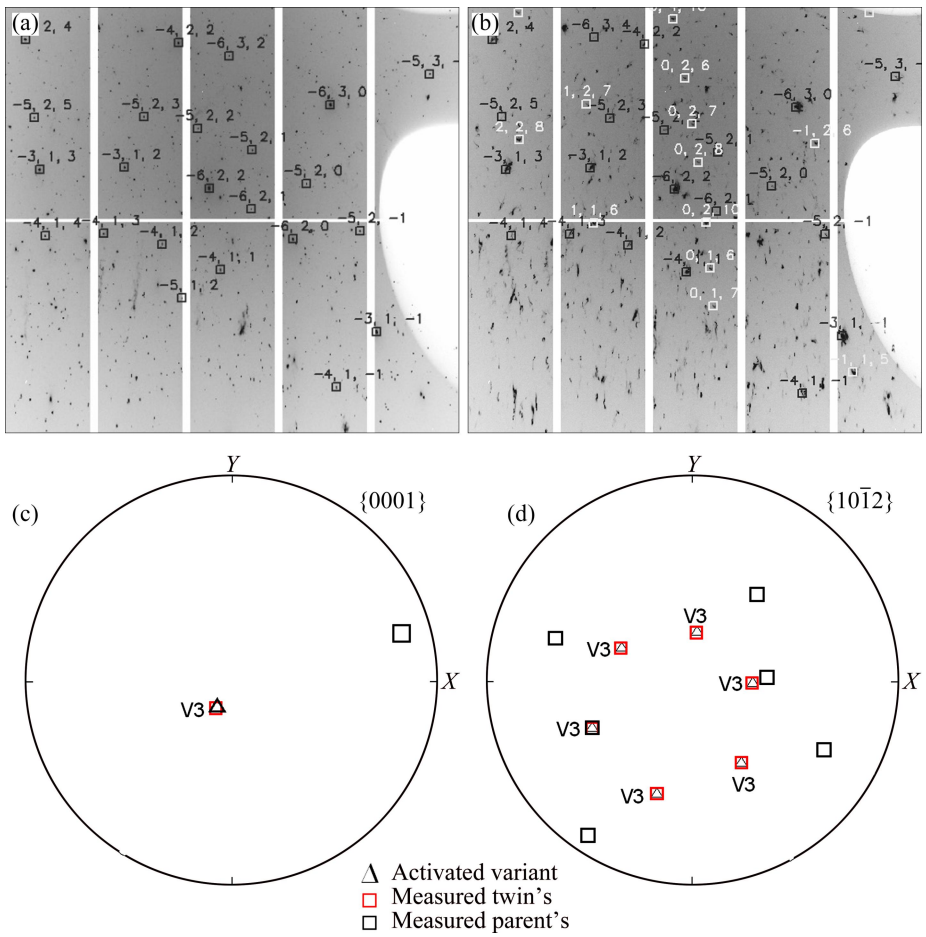

Fig. 6 Crystallographic indexation of parent 192#1 (black) and twin 1−3 (white) for load stage of 68 MPa. Indexations are expressed in Miller-Bravais 3 index. Crystal orientations of parent (a), twin (b) and activated variants are expressed in {0001} pole figure (c) and $\{10\bar{1}2\}$ pole figure (d) (Each pole is labeled by format of "V twin variant No.")

Figures 6(c) and (d) present the crystal orientations of parent, twins and activated variant in pole figures. The {0001} pole figure shows *X* direction, i.e., the tensile direction is approximately parallel to ⟨0001⟩. Actually, this is common characteristics for the identified tensile twins. From $\{10\bar{1}2\}$ pole figure, it can be seen that the poles of theoretical variant match with those of the measured twins at high precision.

Since twinning is seen as dislocation glide for most intents and purposes, actually active twin variants for the identified twins and their Schmid factors were calculated and are listed in Table 1.

Table 1 Activated twin variant and their corresponding Schmid factors

Twin No.	Parent	Active twin variant*	Schmid factor	Highest Schmid factor
1	192#1	Variant 3	0.456	0.456
2	192#1	Variant 3	0.456	0.456
3	192#1	Variant 3	0.456	0.456

*Numbering twin variants is according to Ref. [20].

It has to be pointed out that not all active variants possess the highest Schmid factor. Actually, among the distinguishable 33 grains, there are a couple of grains with more preferred orientation than parent 192#1 for tensile twinning. However, they are free of twin. The results highlight the inability of a simple Schmid factor model to capture the behavior of individual grains. This hypothesis is consistent with the statistic analysis result reported by BEYERLEIN et al [2].

3.2 Observation of twin morphology

Figure 7 illustrates the observation of twin morphology in the sample (*XYZ*) reference frame. Figure 7(a) shows that the crystallographic orientation of the active twin variant within parent 015#6 is expressed in terms of the parent grain orientation (HCP lattice). In Fig. 7(b), the projections of parent grain and its twin in *XOY* plane are presented in gray and RGB colors, while twin's corresponding spheroidal model and its active twin plane are shown in orange and pink color.

Figure 8 presents the evolution of morphologies for

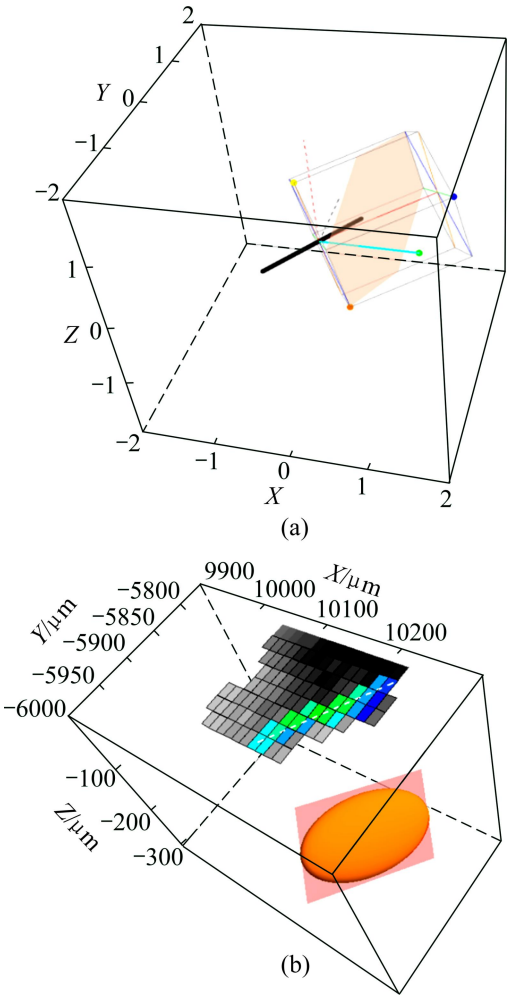

Fig. 7 Observation of twin morphology in sample (*XYZ*) reference frame: (a) Crystallographic orientation of active twin variant in terms of parent 015#6 orientation; (b) Morphology of spheroidal model for twin

three twins within parent 192#1. The reflections of $(22\bar{4}8)$ in all 340 LPs were selected to the morphology maps. The dashed ellipse in each figure highlights the same grain region for each data set. With increasing the load, the spots become streaked or even split.

Figure 9 presents the evolution of 2D morphologies for coexisting three twins (twins 1−3) within one parent grain subjected to different load stages. The parent (gray) gives birth to twin 1 (blue), twin 2 (green) and twin 3 (red). The intensity of $\{22\bar{4}8\}$ reflection was selected to map the morphology of twin. It is shown that the intensity at the middle of trace is higher than that at the tip of twin. The recorded intensity distribution of an individual (*hkl*) Laue reflection arises from the integrated signal along the penetration depth of the incident X-ray beam. The fact means that twins formed is ellipsoidal or disk in shape. It has to be mentioned that three twins develop in nearly same incident angles. The fact is consistent with their common twin variant (Table 1). There is an unconventional fact to be noted that the

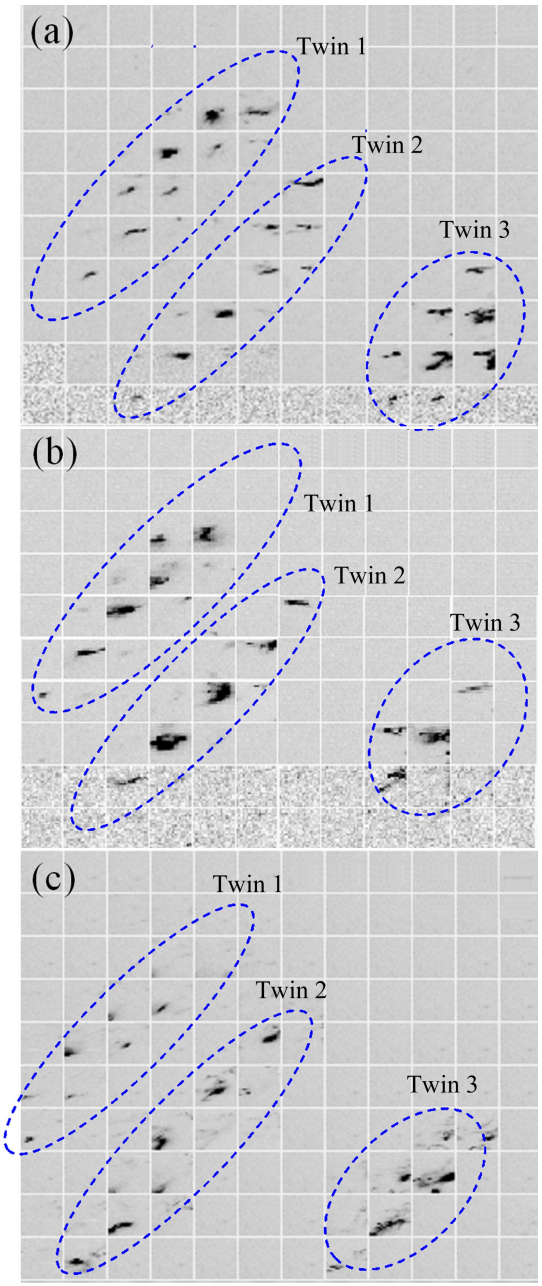

Fig. 8 Evolution of mosaic images for three twins within one parent grain subjected different load stages: (a) 64 MPa; (b) 68 MPa; (c) 73 MPa (Spots are from $(22\bar{4}8)$ reflections)

size of the three twins underwent the bursts of twin growth from 58 MPa to 64MPa. In fact, among the indexed 14 twins, only one twin was found at 58 MPa.

3.3 Evolution of twin misorientation

Figure 10 shows misorientation fluctuations along traces of the three twins. The traces are defined by the yellow lines in Fig. 9. The misorientation between a point on the line and the first point (origin) on the line can be displayed as a function of distance along the line. The misorientation was deduced from orientation

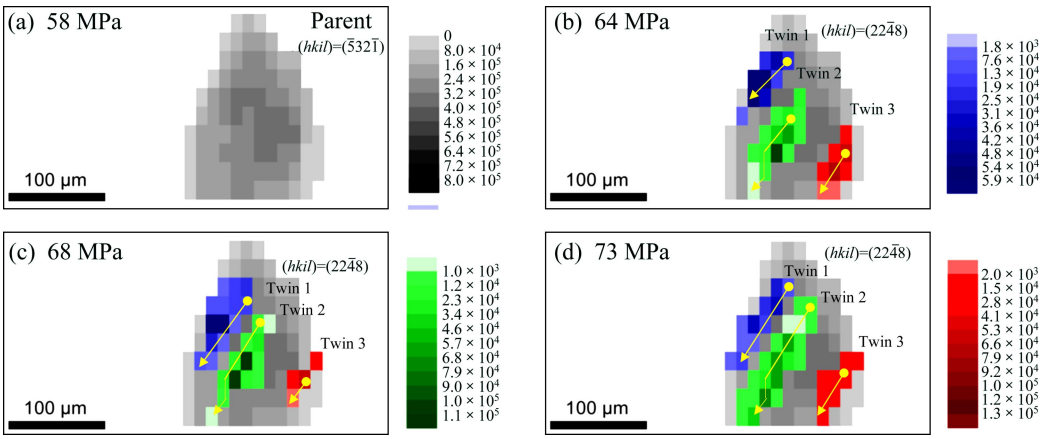

Fig. 9 2D projection of parent grain within mapped X−Y reference frame: (a) Gray scale data signifying intensity data for high-resolution map; (b)−(d) RGB color data signifying intensity data for three twins under three load stages

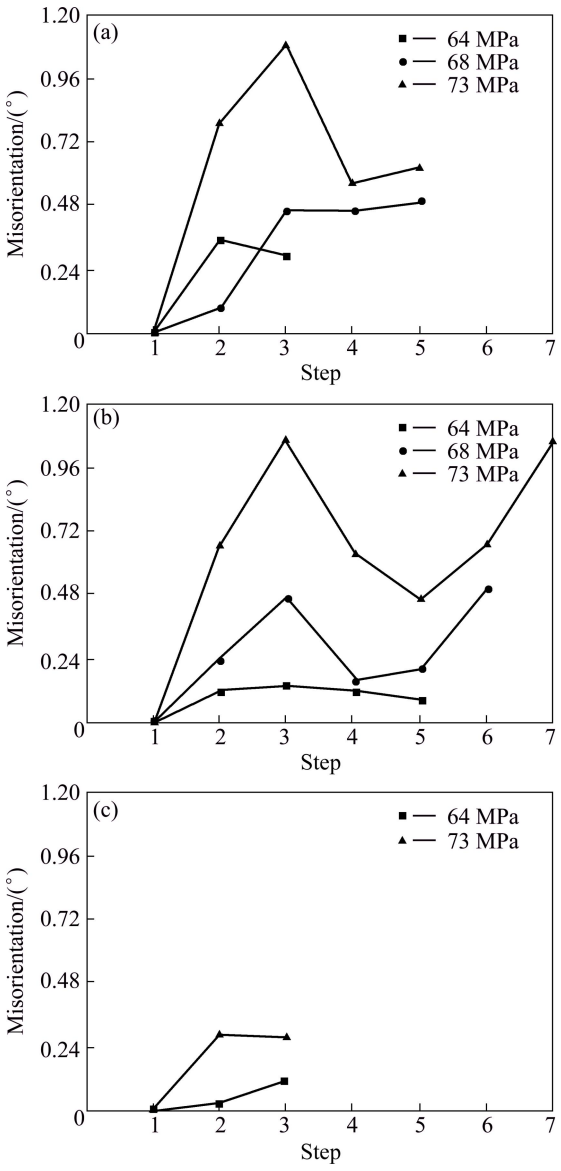

Fig. 10 Evolution of misorientation alone trace for twin 1 (a), 2 (b) and 3 (c) subjected different load stages (Traces are defined by yellow lines in Fig. 9)

matrices for each indexed domain. To guarantee these misorientation curves to be comparable at different loads, the origin points were fixed at the same position. Noting that continuous tests were carried out and the loads were held at the designed levels, the deformation of the crystalline was also in succession. The misorientation angle of the twins can not be assessed separately at the given load without by-past data. However, the misorientation angles of one twin at different load levels are comparable and make sense. As load increases, the amplitude of misorientation within one twin basically increases and fluctuates more sharply. The local misorientation increasing can be attributed to the accumulation of geometrically necessary dislocations [21]. Therefore, the distribution of strain is highly inhomogenous during twin propagation.

3.4 Evolution of twin mosaic spread

Figures 11(a)−(c) present the mosaicity spread of twins 1, 2 and 3 by quantitatively expressing their streaking of diffraction spot (22$\bar{4}$8) along vertical direction. Figure 11(d) illustrates that the mosaic spread of diffraction spot was evaluated by its vertical width. At the load stage of 64 MPa, the tips of twins occur more substantial mosaic spread, compared with the middle of twins. As the load increases, the mosaicity in the middle twins tends to be more serious. During plastic deformation, the formation of highly correlated unpaired GND and geometrically necessary boundaries (GNB) can lead to long-range lattice rotations at the sub-grain level. Subsequent lattice rotation (misorientation) is observed experimentally in polychromatic micro-XRD as streaking (broadening) or even splitting of individual Laue reflections. Thus, with increasing the load, the substantial mosaicity is consistent with the amplitude of misorientation fluctuation (Fig. 10).

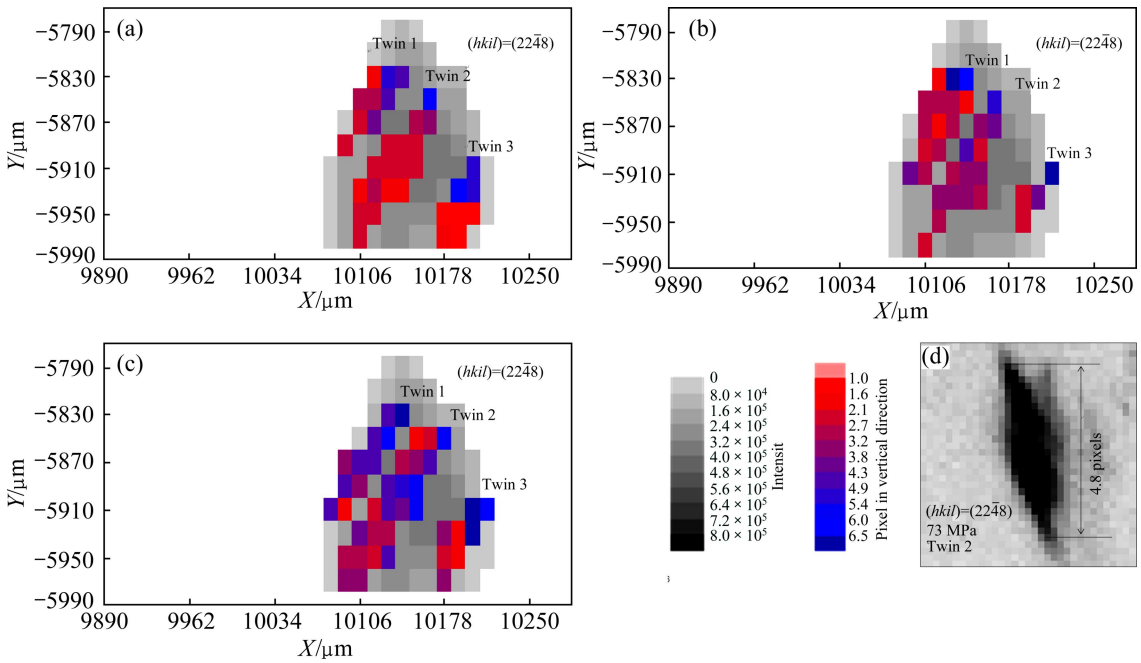

Fig. 11 Observation of mosaicity of twins 1, 2 and 3 by quantitatively expressing their streaking of diffraction spot $(22\bar{4}8)$ along vertical direction at three load levels: (a) 64 MPa; (b) 68 MPa; (c) 73 MPa (Scheme of mosaicity evaluation is illustrated in (d) for twin 2 at 73 MPa)

4 Conclusions

1) An important method to detect the misorientation quantitatively in the polycrystalline materials is illustrated.

2) For the deformation twinning process activated by stress concentration, 14 twins are identified and twin statistics are improved with semi-automated approach within the area of 396 μm × 200 μm.

3) As the load increases, the amplitude of misorientation fluctuation along twin trace keeps increasing. The increase of local misorientation can be attributed to the accumulation of GND.

Acknowledgements

The author would like to gratefully thank associated Prof. Peter LYNCH and Prof. Matthew BARNETT, Institute for Frontier Materials, Deakin University, for their experimental supports and directions.

References

[1] BETTLES C, BARNETT M. Advances in wrought magnesium alloys: Fundamentals of processing, properties and applications [M]. Cambridge: Woodhead Publishing Limited, 2012: 480.

[2] BEYERLEIN I J, CAPOLUNGO L, MARSHALL P E, McCABE R J, TOME C N. Statistical analyses of deformation twinning in magnesium [J]. Philos Mag, 2010, 90(16): 2161−2190.

[3] LAN Y T, ZHONG X C, QUAN G F, LIN R C, ZHANG K S. Crystal anisotropy of AZ31 magnesium alloy under uniaxial tension and compression [J]. Transactions of Nonferrous Metals Society of China, 2015, 25(1): 249−260.

[4] MURAŇSK O, CARR D G, ŠITTNER P, OLIVER E C. In situ neutron diffraction investigation of deformation twinning and pseudoelastic-like behaviour of extruded AZ31 magnesium alloy [J]. Int J Plast, 2009, 25(6): 1107−1127.

[5] AGNEW S R, BROWN D W, TOME´ C N. Validating a polycrystal model for the elastoplastic response of magnesium alloy AZ31 using in situ neutron diffraction [J]. Acta Mater, 2006, 54(18): 4841−4852.

[6] MURÁNSKY O, BARNETT M R, LUZIN V, VOGEL S. On the correlation between deformation twinning and Lüders-like deformation in an extruded Mg alloy: In situ neutron diffraction and EPSC.4 modelling [J]. Materials Science and Engineering A, 2012, 527(6): 1383−1394.

[7] LARSON B C, YANG W, ICE G E, BUDAI J D, TISCHLER J Z. Three-dimensional X-ray structural microscopy with submicrometre resolution [J]. Nature, 2002, 415(6874): 887−890.

[8] AYDINER C C, BERNIER J V, CLAUSEN B, LIENERT U, TOME C N, BROWN D W. Evolution of stress in individual grains and twins in a magnesium alloy aggregate [J]. Phys Rev B, 2009, 80(2): 024113.

[9] BARABASH R I, ICE G E, LIU W, BARABASH O M. Polychromatic microdiffraction characterization of defect gradients in severely deformed materials [J]. Micron, 2009, 40(1): 28−36.

[10] LYNCH P A, TOMUS D, BETTLES C J, GIBSON M A, STEVENSON A W. A comparative EBSD and micro-XRD study of the intergranular grain structure in CP-Ti [J]. Nucl Instrum Meth Phys Res A, 2010, 619(11): 298−301.

[11] BALOGH L, NIEZGODA S R, KANJARLA A K, BROWN D W, CLAUSEN B, LIU W, TOME C N. Spatially resolved in situ strain measurements from an interior twinned grain in bulk polycrystalline AZ31 alloy [J]. Acta Mater, 2013, 61(10): 3612−3620.

[12] ODDERSHEDE J, CAMIN B, SCHMIDT S, MIKKELSEN L P, SϕRENSEN H O, LIENERT U, POULSEN H F, REIMERS W. Measuring the stress field around an evolving crack in tensile

deformed Mg AZ31 using three-dimensional X-ray diffraction [J]. Acta Mater, 2012, 60(8): 3570−3580.
[13] ASHBY M F. Deformation of plastically non-homogeneous materials [J]. Philos Mag, 1970, 21: 399−424.
[14] KHOSRAVANI A, SCOTT J, MILES M P, FULLWOOD D, ADAMS B L, MISHRA R K. Twinning in magnesium alloy AZ31B under different strain paths at moderately elevated temperatures [J]. Int J Plast, 2013, 45: 160−173.
[15] PROUST G, TOME C N, KASCHNER G C. Modeling texture, twinning and hardening evolution during deformation of hexagonal materials [J]. Acta Mater, 2007, 55(6): 2137−2148.
[16] LYNCH P A, KUNZ M, TAMURA N, BARNETT M R. Time and spatial resolution of slip and twinning in a grain embedded within a magnesium polycrystal [J]. Acta Mater, 2014, 78: 203−212.
[17] TAMURA N, MACDOWELL A A, SPOLENAK R, VALEK B C, BRAVMAN J C, BROWN W L, CELESTRE R S, PADMORE H A, BATTERMAN B W, PATEL J R. Scanning X-ray microdiffraction with submicrometer white beam for strain/stress and orientation mapping in thin films [J]. J Synchrotron Radiat, 2003, 10: 137−143.
[18] TAMURA N, KUNZ M, CHEN K, CELESTRE R S, MACDOWELL A A, WARWICK T. A superbend X-ray microdiffraction beamline at the advanced light source [J]. Mater Sci Eng A, 2009, 524(1−2): 28−32.
[19] BARABASH R I, ICE G E, PANG J W L. Gradients of geometrically necessary dislocations from white beam microdiffraction [J]. Mater Sci Eng A, 2005, 400−401: 125−131.
[20] CHENEAUSPATH N, FILLIT R Y, DRIVER J H. Improved X-ray and electron-diffraction methods for twin determination in hexagonal crystals [J]. J Appl Crystallogr, 1994, 27: 980−987.
[21] BARABASH R I, ICE G E, LIU W J, BARABASH O M. Polychromatic microdiffraction characterization of defect gradients in severely deformed materials [J]. Micron, 2009, 40(1): 28−36.

基于同步辐射连续 X 射线谱的多重孪生形态与长大的原位分析

李 理[1,2]

1. 湖南工学院 先进制造技术研究所，衡阳 421002；
2. Institute for Frontier Materials, Deakin University, Geelong, Victoria 3220, Australia

摘 要：同步辐射连续 X 射线谱微衍射技术被应用于原位研究 AZ31 (Mg−3Al−1Zn)薄板单向拉伸过程中的形变孪生，对孪晶在 64~73 MPa 载荷条件下的形态和生长进行原位分析。在先进光源中心(ALS)的 12.3.2 光束线采集的 X 射线衍射数据被用来表征面积为 396 μm × 200 μm 的关注区域。该实验装置和具有深度分辨能力的 X 射线显微术可在亚微米尺度上确定晶粒内位置与取向联系。一系列基体晶粒按照晶体取向分类来研究孪生行为。结果展示了相同晶粒内多重孪生的孪生变体选择、局域取向差波动及镶嵌块扩展。随着载荷增加，沿孪晶迹线方向的取向差波动持续增加，其原因归结为几何必需位错的积累。

关键词：同步辐射 X 射线；形变孪生；原位分析；局域取向差；几何必需位错

(Edited by Mu-lan QIN)